Adsorption of hydrogen atoms on the Si(100)-2×1 surface: implications for the H_2 desorption mechanism

Christine J. Wu and Emily A. Carter

Department of Chemistry and Biochemistry, University of California, Los Angeles, CA 90024-1569, USA

Received 5 August 1991

The adsorption of atomic hydrogen on the reconstructed Si(100)-2×1 surface is studied using embedded Si clusters as models of an extended Si surface. Analytic gradients of generalized valence bond (GVB) wavefunctions are used to predict equilibrium structures and harmonic vibrational frequencies; the correlation-consistent configuration interaction (CCCI) method is used to calculate heats of adsorption. We predict that the first Si–H bond strength of a silicon dimer D_0(Si–Si–H) is 86.1 kcal/mol, while the second Si–H bond strength D_0(HSiSi–H) is 87.9 kcal/mol. Thus, no significant thermodynamic preference exists for either Si–Si–H or H–Si–Si–H surface configurations, consistent with recent infrared and scanning tunneling microscopy experiments. The predicted adsorption energetics have important consequences for H_2 desorption (ΔE_{des} = 70.7 kcal/mol), with a new mechanism proposed involving H atom diffusion followed by pre-pairing desorption of two H atoms on adjacent silicon dimers in the same dimer row.

1. Introduction

The interaction of hydrogen with the Si(100) surface has been the object of intense research recently because of its important role in several surface chemical reactions such as chemical vapor deposition of silicon from silane [1], oxidation of silicon by H_2O [2], and nitridation of silicon by NH_3 [3,4]. The Si(100)-2×1 surface is characterized by the formation of symmetric Si dimers, observed experimentally by scanning tunneling microscopy (STM) [5,6] and predicted even earlier by theory [7]. During the surface reconstruction, each surface Si atom forms a σ bond with an adjacent Si atom and leaves two weakly coupled dangling bonds on the incipient dimer, leading to the observed p(2×1) surface symmetry. Adsorption of H atoms on this surface results in saturation of the dangling bonds of silicon dimers to form a stable p-(2×1)-monohydride phase [8–18].

Experimental characterization of this monohydride phase has primarily consisted of vibrational spectroscopy [12–14], H_2 desorption kinetic studies [19–21], and more recently STM [22] and resonance-enhanced multiphoton ionization (REMPI) [23]. Fourier transform infrared (FT-IR) [12,13] and high resolution electron energy loss (HREELS) [14] spectroscopies have identified monohydride stretching and bending frequencies at ≈2080–2095 cm^{-1} and 630 cm^{-1}, respectively. Two different groups have measured the H_2 desorption kinetics from the monohydride phase, each with laser-induced thermal desorption (LITD) and temperature-programmed desorption (TPD) [19–21]. Sinniah et al. [19,20] measured the desorption activation energy, E_{des}, to be 45±2 kcal/mol by LITD and 50±2 kcal/mol by TPD. By contrast, Wise et al. [21] found E_{des} to be 58±2 kcal/mol by LITD and 66±4 kcal/mol by TPD. It is clear from both the conflict-

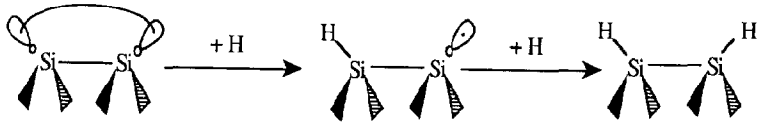

ing data and subsequent interpretations (vide infra) that the desorption mechanism and its associated energetics are far from unequivocally determined. In order to help sort out these issues, this Letter describes a theoretical characterization of the H atom adsorption energetics on the Si(100)-2×1 surface.

Previous theoretical calculations on the monohydride phase have focused on predicting the valence band density of states [24], equilibrium geometries [13,24–26] and vibrational properties [13] using self-consistent band theory [24], semi-empirical methods [25,26], and perturbation theory [13]. The Si–Si and Si–H bond lengths in the hydrogenated dimer have been predicted semi-empirically to be R_e(Si–Si) = 2.53 or 2.37 Å and R_e(Si–H) = 1.49 or 1.53 Å, using either a cluster [25] or a slab [26] surface model, respectively. Ab initio perturbation theory [13] predicted R_e(Si–Si) = 2.51 Å, R_e(Si–H) = 1.48 Å, and $\theta_{H\text{–}Si\text{–}Si} = 110°$. In this same work, vibrational frequency shifts and dynamics dipole moments were calculated to be in good agreement with FT-IR measurements [13]. The only theoretical energetics reported to date is a lower bound for E_{des} of 19 kcal/mol, from semi-empirical MINDO/3 calculations [25]. However, MINDO/3 is not expected to provide reliable energetics, since it is only an approximation to ab initio Hartree–Fock (HF) theory, which is known to predict energetics extremely poorly.

In order to obtain quantitative adsorption energies for the monohydride phase, more accurate ab initio techniques need to be employed. In this paper, we report highly correlated ab initio calculations of the Si–H geometries, vibrational frequencies, and bond dissociation energies for the monohydride phase of the Si(100) surface. Our predictions for the heats of adsorption are then used to discuss the desorption mechanism for the monohydride phase (β_1 desorption).

2. Calculational details

The smallest repeat unit on a Si(100)-2×1 surface is an Si dimer. Thus, our cluster model contains one surface dimer, its four nearest-neighbor atoms in the second layer, two third layer neighbor atoms connected to the four atoms in the second layer and one fourth layer neighbor atom connected to the two third layer atoms, for a total of nine Si atoms. In order to model an extended lattice structure, it is necessary to embed this nine atom Si cluster so that the subsurface Si atoms remain tetravalent and hence approximately bulk-like. Thus, all the dangling bonds of subsurface Si atoms are saturated by modified H atoms ($\bar{H}$), described by a basis set adjusted to have the same electronegativity as bulk Si atoms [7,27]. This embedding procedure gives rise to an $Si_9\bar{H}_{12}$ cluster model

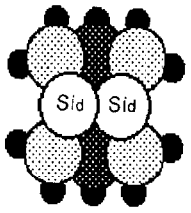

with a charge distribution and hybridization that should resemble the extended surface. Effective core potentials and valence double zeta basis sets were used to represent the core and valence electrons of all Si atoms [28], respectively. In addition, one set of 3d polarization functions ($\zeta^d = 0.3247$) were added to each surface Si atom. The chemisorbed H atoms were described by the Dunning triple-zeta contraction [29] of the Huzinaga 6s Gaussian basis set [30], with one set of 2p polarization functions ($\zeta^p = 0.6$) added.

Self-consistent field (SCF) orbital optimization of the Si–H bonds and the Si–Si dimer bond were performed at the generalized valence bond with perfect singlet pairing (GVB-PP) level [31], while all other orbitals were treated at the HF level. Si–H bond dissociation energies were calculated using the GVB-CCCI method [32,33], which is a nearly size-consistent multireference configuration interaction approach that includes all single and double excitations from the breaking bond pairs (one pair at a time) and single excitations from all valence orbitals. Typical accuracies of within 2 kcal/mol of experiment are routinely achieved by this method for single bond strengths in main group molecules [27,32–35].

The equilibrium geometries and vibrational frequencies for the monohydride phase were obtained from analytic gradients [36,37] of GVB-PP wavefunctions for the $Si_9\bar{H}_{12}H$ and $Si_9\bar{H}_{12}H_2$ clusters. At

present, it is not computationally feasible to perform the higher level CI calculations (CCCI) on clusters of the size of $Si_9\bar{H}_{12}H$ and $Si_9\bar{H}_{12}H_2$. Since the CI calculations must therefore be performed on smaller clusters, we have devised a geometry mapping procedure to take the optimized structures from the large clusters and map them onto smaller geometry-mapped (GM) clusters ($Si_2\bar{H}_4H$ and $Si_2\bar{H}_4H_2$). In particular, these clusters are constructed by keeping the same geometry of the top two layers of $Si_9\bar{H}_{12}H$ and $Si_9H_{12}H_2$, with the Si–$\bar{H}$ distance fixed at 1.729 Å (taken from the Si–$\bar{H}$ bond length in the optimized larger clusters). The error introduced by this transformation is small ($\approx$2 kcal/mol) [27], since the actual interactions between the incoming H atoms and the surface Si atoms are localized to the surface anyway. The resulting surface wavefunctions for both the large and small clusters are nearly identical [27], lending support to the use of such geometry mappings. Subsequently, the CCCI calculations are carried out on the smaller GM $Si_2\bar{H}_4H$ and $Si_2\bar{H}_4H_2$ clusters to obtain the Si–H bond strengths for the monohydride phase.

3. Results and discussion

Adsorption of the first H atom onto a bare Si dimer leads to an Si–Si–H surface species. Gradient optimization of the $Si_9\bar{H}_{12}H$ cluster yields $R_e(Si_d–Si_d)=2.44$ Å, $R_e(Si_d–Si_{sub})=2.36$ Å, $R_e(Si_d–H)=1.51$ Å, and $\theta_{H–Si_d–Si}=114.0°$ (where Si_d is a silicon dimer atom and Si_{sub} a subsurface Si atom), similar to previous studies [13]. The predicted harmonic stretching frequency of the Si–H bond is 2247 cm^{-1}. The heat of adsorption of the first H atom added to an Si dimer obtained from both the larger $Si_9\bar{H}_{12}H$ cluster and the smaller GM $Si_2\bar{H}_4H$ cluster calculations are listed in tables 1 and 2, respectively. Our best level of calculation (CCCI) yields a first Si–H bond strength of $D_0=86.1$ kcal/mol.

Adsorption of the second H atom onto a partially hydrogenated dimer (Si–Si–H) yields the fully saturated dimer. The one-electron GVB orbitals for the Si–Si dimer and the Si–H bonds are depicted in fig. 1. The Si–H bond is strongly covalent, with one electron localized on H and one electron in an Si sp^3-like hybrid orbital. The partially hydrogenated dimer (Si–Si–H) orbitals look essentially identical to these, with the singly occupied dangling bond remaining localized as in the Si orbital in fig. 1a. Optimization of $Si_9\bar{H}_{12}H_2$ yields a similar geometry to the partially hydrogenated dimer: $R_e(Si_d–Si_d)=2.43$ Å, $R_e(Si_d–Si_{sub})=2.36$ Å, $R_e(Si_d–H)=1.51$ Å, and $\theta_{H–Si_d–Si_d}=114.7°$. The symmetric and antisymmetric Si–H harmonic stretching vibrations are predicted to be 2063 and 2244 cm^{-1}, respectively, in reasonable agreement with experiment (2080–2095 cm^{-1}) [12–14]. The Si–H bond strength calculated from both $Si_9\bar{H}_{12}H_2$ and GM $Si_2\bar{H}_4H_2$ clusters are displayed in tables 1 and 2, respectively. The CCCI calculation predicts the heat of adsorption of an H atom to a partially hydrogenated dimer (Si–Si–H) to be $D_0=87.9$ kcal/mol, slightly larger than for the first H atom to adsorb.

Table 1
Equilibrium properties of the optimized $Si_9\bar{H}_{12}H$ and $Si_9\bar{H}_{12}H_2$ clusters at the GVB-PP level

Properties	$Si_9\bar{H}_{12}H$	$Si_9\bar{H}_{12}H_2$
bond energies (kcal/mol) [a]		
D_e (Si–H) [b]	79.3	79.6
D_0 (Si–H) [c]	71.3	77.6
vibrational frequencies (cm^{-1})		
Si–H stretching	2247	2063, 2244
geometries (Å, deg)		
$R_e(Si_d–H)$	1.51	1.51
$R_e(Si_d–Si_d)$	2.44	2.43
$R_e(Si_d–Si_{sub})$	2.36	2.36
$\theta_{H–Si_d–Si_d}$	114.0	114.7

[a] The total energies for the H atom, the optimized $Si_9\bar{H}_{12}(^1A_1)$, $Si_9\bar{H}_{12}H$ ($^2A'$) and $Si_9\bar{H}_{12}H_2(^1A_1)$ clusters at the GVB-PP level used here are −0.49994, −2605.22127, −2605.84781 and −2606.47469 hartree, respectively. 1 hartree = 627.5096 kcal/mol = 27.21162 eV = 219474.8 cm^{-1}. Equilibrium geometries optimized at the GVB-PP level are used for all molecules (see text).

[b] $D_e(Si_9\bar{H}_{12}–H)=E(Si_9\bar{H}_{12}H, {}^2A')-E(Si_9\bar{H}_{12}, {}^1A_1)$ = the adiabatic bond dissociation energy associated with the first H atom to adsorb. $D_e(Si_9\bar{H}_{12}, H–H)=E(Si_9\bar{H}_{12}H_2, {}^1A_1)-E(Si_9\bar{H}_{12}H, {}^2A')$ = the adiabatic bond dissociation energy associated with the second H atom to adsorb.

[c] Theoretical zero-point energies (ZPE) of 69.8, 77.8 and 79.8 kcal/mol for the optimized $Si_9\bar{H}_{12}(^1A_1)$, $Si_9\bar{H}_{12}H$ (2A′) and $Si_9\bar{H}_{12}H_2$ ($^1A_1$) clusters were used to convert D_e to D_0, respectively.

Table 2
The first (top) and second (bottom) Si–H bond dissociation energies (kcal/mol) obtained from the GM $Si_2\bar{H}_4H$ and $Si_2\bar{H}_4H_2$ clusters calculations

Calculation [a]	Total energies (hartree)		D_e ($Si_2\bar{H}_4$–H) [b]	D_0($Si_2\bar{H}_4$–H) [c]
	$Si_2\bar{H}_4H$ ($^2A'$)	$Si_2\bar{H}_4$ ($^3B_1$)		
GVB(2/4)-PP	−580.16574 (4/4)	−579.53786 (2/2)	79.8	
GVB-RCI(2/4)	−580.16596 (9/17)	−579.53794 (4/4)	79.8	
CCCI(2/4)	−580.20341 (1688/5349)	−579.55278 (192/432)	94.1	86.1
Calculation [a]	Total energies (hartree)		D_e ($Si_2\bar{H}_4H$–H) [d]	D_0($Si_2\bar{H}_4H$–H) [c]
	$Si_2\bar{H}_4H_2$ ($^1A_1$)	$Si_2\bar{H}_4H$ ($^2A'$)		
GVB(3/6)-PP	−580.79403 (8/8)	−580.16574 (4/4)	80.5	
GVB-RCI(3/6)	−580.79457 (27/37)	−580.16596 (9/17)	80.7	
CCCI(3/6)	−580.83132 (6169/12819)	−580.18817 (947/3393)	89.9	87.9

[a] The corresponding number of spatial configurations/spin eigenfunctions for each wavefunction are given beneath each total energy. The geometries of GM $Si_2\bar{H}_4$, $Si_2\bar{H}_4H$ and $Si_2\bar{H}_4H_2$ clusters were taken from the optimized $Si_9\bar{H}_{12}$, $Si_9\bar{H}_{12}H$ and $Si_9\bar{H}_{12}H_2$ clusters (see text).

[b] $D_e(Si_2\bar{H}_4\text{–H}) = E(Si_2\bar{H}_4\text{–H}, {}^2A') - E(Si_2\bar{H}_4, {}^3B_1) - \Delta E_{ST}$, where $\Delta E_{ST} = E(Si_2\bar{H}_4, {}^1A_1) - E(Si_2\bar{H}_4, {}^3B_1) = 0.58$ kcal/mol (see ref. [32] for details).

[c] Theoretical zero-point energies (ZPE) of 69.8, 77.8 and 79.8 kcal/mol for the optimized $Si_9\bar{H}_{12}$ ($^1A_1$), $Si_9\bar{H}_{12}H$ ($^2A'$) and $Si_9\bar{H}_{12}H_2$ ($^1A_1$) clusters were used to convert D_e to D_0, respectively.

[d] D_e ($Si_2\bar{H}_4H$–H) = $E(Si_2\bar{H}_4H_2, {}^1A_1) - E(Si_2\bar{H}_4H, {}^2A')$.

We find the intrinsic stability of an H–Si–Si species to be essentially the same (within 2 kcal/mol) as an H–Si–Si–H species. We note that, simultaneous with our work, Nachtigall et al. have used quadratic CI to obtain somewhat lower and more differentiated Si–H bond strengths: 76 and 81 kcal/mol for the first and second Si–H bonds in the Si_9H_{13} and Si_9H_{14} clusters, respectively [38]. At low hydrogen coverage, FT-IR experiments of Chabal et al. indicate that the vibrational spectrum is inhomogenously broadened [12], which may be due to H atoms randomly adsorbing onto empty sites of the Si(100)-2×1 surface with no preferred order, consistent with our finding that the first Si–H bond is nearly as strong as the second Si–H bond formed with a surface dimer. Recent STM studies also observe a random adsorption pattern at low temperature, while at high temperature H–Si–Si–H species appear to dominate when the barrier to diffusion can be overcome [22]. Since the Si–H bond strengths are essentially the same, providing no large thermodynamic driving force for pairing up the H atoms, Boland has suggested [22] that pairing of dimer dangling bond orbitals may be the driving force for formation of H–Si–Si–H. However, our calculations and previous ones [7] suggest that this coupling is very weak ($\approx$1–2 kcal/mol). Thus, it may be that a small driving force of $\approx$4 kcal/mol per pair of H atoms and pair of dimers is enough to favor formation of H–Si–Si–H (adding the differential bond strengths and the dangling bond coupling together). Otherwise, long range effects such as lattice strain may also contribute to site occupation preferences.

The total heat of adsorption for the fully saturated monohydride phase (θ_H=1.0) is predicted to be 86.1+87.9=174.0 kcal/mol downhill. Thus, the en-

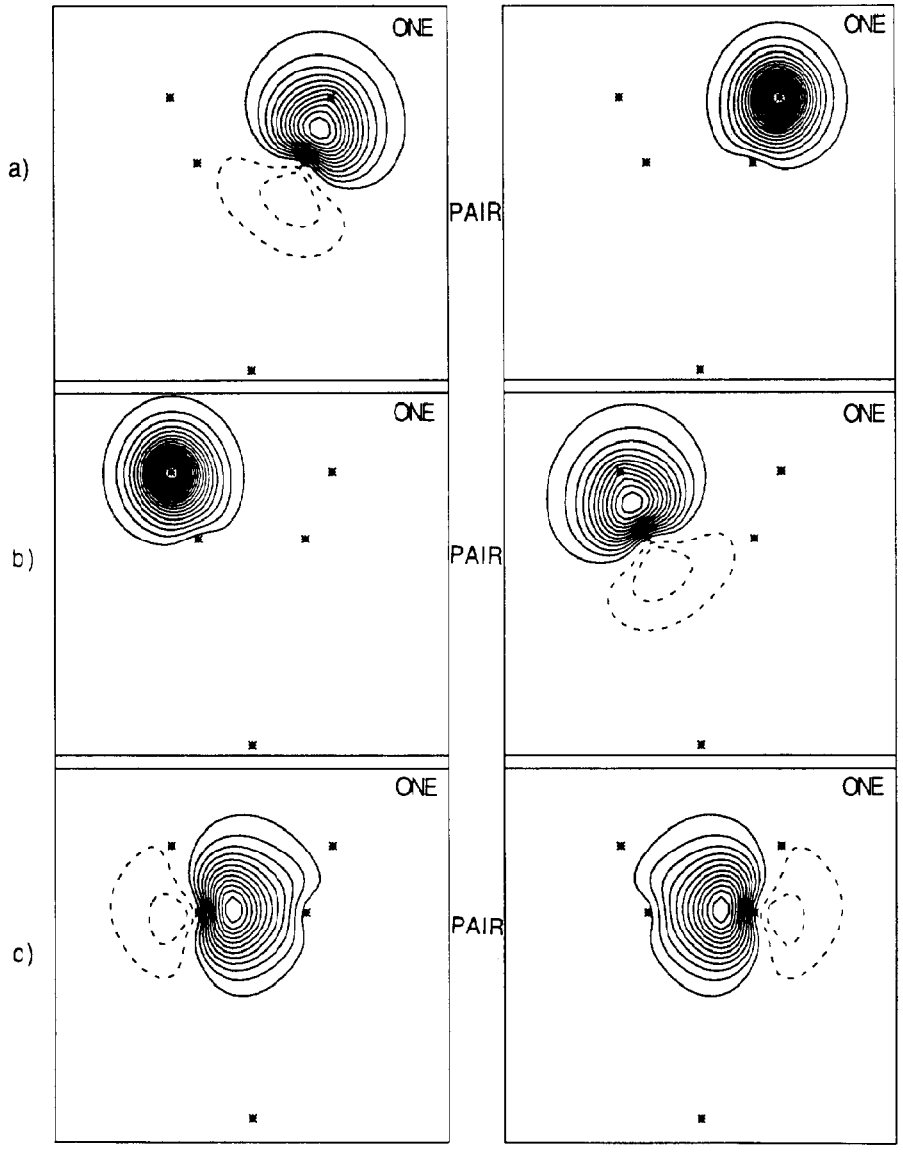

Fig. 1. Contour maps of one-electron GVB orbitals for the optimized $Si_9\bar{H}_{12}H_2$ cluster: (a) the right Si–H bond pair (overlap=0.813); (b) the identical left Si–H bond pair; (c) the Si–Si dimer σ bond pair (overlap=0.828).

dothermicity for H_2 desorption from this phase, ΔE_{des}, is predicted to be 174.0 − 103.3 = 70.7 kcal/mol, using the known bond dissociation energy (D_0) of H_2 [39]. Since all of the experimental measurements of the desorption activation barrier, E_{des}, range from only 45 to 66 kcal/mol, which are lower than our predicted ΔE_{des}, we conclude that the desorption process is not direct, but must include at least two steps. Sinniah et al. [19,20] proposed a two-step desorption mechanism involving an irreversible excitation of $H_{(a)}$ to a two-dimensional delocalized band state as the rate limiting step. However, this proposed mechanism directly conflicts the recent experimental observation that H_2 is rotationally cold

after it is thermally desorbed from the Si(100) surface [23]. Furthermore, Sinniah's model implies that the H_2 desorption mechanism is independent of surface structure, inconsistent with studies of the thermal desorption of H_2 from Si(111)-7×7, which exhibited different kinetics from Si(100)-2×1 (second order versus first order kinetics) [19–21]. Very recently, Wise et al. proposed a "pre-pairing" desorption mechanism involving two hydrogen atoms on the same dimer, in order to explain the observation of first order kinetics for H_2 desorption from the Si(100)-2×1 surface. However, our preliminary calculations on the desorption process [40] show that H_2 desorption from two H atoms on the same dimer has a very large activation energy ($\approx$120 kcal/mol) and hence is unlikely to be the H_2 desorption pathway. Instead, analogous calculations [40] on H atom diffusion suggest that H_2 may desorb from two prepaired H atoms on the same side of two adjacent silicon dimers in the same row. Our calculations on hydrogen diffusion on the Si(100)-2×1 surface also indicate that the diffusion activation energy falls in the range of reported desorption barriers, implying that diffusion of H atoms will occur simultaneous with desorption of H_2. Thus, a likely desorption scenario consists of a pre-equilibrium step involving H atom diffusion, leading to an apparent activation energy that is actually the difference between E_{des} and E_{diff}. In particular, H atom diffusion may be necessary to set up "pre-pairing" for desorption. Explicit theoretical investigations of hydrogen desorption from the monohydride phase are in progress.

Acknowledgement

We are grateful to the Air Force Office of Scientific Research (Grant. No. AFOSR-89-0108) for generous support of this work. EAC also acknowledges the National Science Foundation and the Camille and Henry Dreyfus Foundation for partial support this work through their Presidential Young Investigator and Distinguished New Faculty Award Programs, respectively. CJW is grateful for a Products Research Corporation Prize for Excellence in Research.

References

[1] F. Bozso and P. Avouris, Appl. Phys. Letters 53 (1988) 1095.
[2] H. Ibach, H. Wagner and D. Bruchmann, Solid State Commun. 42 (1982) 457.
[3] L. Kubler, E.K. Hlil, D. Bolmont and G. Gewinner, Surface Sci. 183 (1987) 503.
[4] R.J. Hamers, P. Acouris and F. Bozso, Phys. Rev. Letters 59 (1987) 2071.
[5] R.M. Tromp, R.J. Hamers and J.E. Demuth, Phys. Rev. Letters 55 (1985) 1303.
[6] R.M. Tromp, R.J. Hamers and J.E. Demuth, Phys. Rev. B 34 (1986) 5343.
[7] A. Redondo and W.A. Goddard III, J. Vacuum Sci. Technol. 21 (1982) 344.
[8] H. Ibach and J.E. Rowe, Surface Sci. 43 (1974) 481.
[9] T. Sakurai and H.D. Hagstrum, Phys. Rev. B 14 (1976) 1593.
[10] S. Maruno, H. Iwasaki, K. Honrioka, S. Li and S. Nakamura, Surface Sci. 123 (1982) 18.
[11] K. Fujiwara, Phys. Rev. B 26 (1982) 2036.
[12] Y.J. Chabal, E.E. Chaban and S.B. Christman, J. Electron Spectry. Relat. Phenom. 29 (1983) 35.
[13] Y.J. Chabal and K. Raghavachari, Phys. Rev. Letters 53 (1984) 282.
[14] R. Butz, E.M. Oellig, H. Ibach and H. Wagner, Surface Sci. 147 (1984) 343.
[15] S. Ciraci, R. Butz, E.M. Oellig and H. Wagner, Phys. Rev. B 30 (1984) 711.
[16] J.A. Schaefer, F. Stucki, D.J. Frankel, W. Gopel and G.J. Lapeyre, J. Vacuum Sci. Technol. B 2 (1984) 359.
[17] J.J. Boland, Phys. Rev. Letters 65 (1990) 3325.
[18] K. Oura, J. Yamane, K. Umezawa, M. Naitoh, F. Shoji and T. Hanawa, Phys. Rev. B 41 (1990) 1200.
[19] K. Sinniah, M.G. Sherman, L.B. Lewis, W.H. Weinberg, J.T. Yates Jr. and K.C. Janda, Phys. Rev. Letters 62 (1989) 567.
[20] K. Sinniah, M.G. Sherman, L.B. Lewis, W.H. Weinberg, J.T. Yates Jr. and K.C. Janda, J. Chem. Phys. 92 (1990) 5700.
[21] M.L. Wise, B.G. Koehler, P. Gupta, P.A. Coon and S.M. George, submitted for publication.
[22] J.J. Boland, submitted for publication.
[23] K.W. Kolasinski, S.F. Shane and R.N. Zare, submitted for publication.
[24] J.A. Appelbaum, G.A. Baraff, D.R. Hamann, H.D. Hagstrum and T. Sakurai, Surface Sci. 70 (1978) 654.
[25] W.S. Verwoerd, Surface Sci. 108 (1981) 153.
[26] B.I. Craig and P.V. Smith, Surface Sci. 226 (1990) L55.
[27] C.J. Wu and E.A. Carter, to be submitted.
[28] A.K. Rappé, T.A. Smedley and W.A. Goddard III, J. Phys. Chem. 85 (1981) 1662.
[29] T.H. Dunning Jr., J. Chem. Phys. 53 (1970) 2823.
[30] S. Huzinaga, J. Chem. Phys. 42 (1965) 1293.
[31] F.W. Bobrowicz and W.A. Goddard III, Methods of electronic structure theory, Vol. 3 (Plenum Press, New York, 1977).

[32] E.A. Carter and W.A. Goddard III, J. Chem. Phys. 88 (1988) 3132.
[33] E.A. Carter and W.A. Goddard III, J. Chem. Phys. 88 (1988) 1752.
[34] C.J. Wu and E.A. Carter, J. Am. Chem. Soc. 112 (1990) 5893.
[35] C.J. Wu and E.A. Carter, J. Phys. Chem. (1991), in press.
[36] H.B. Schlegel, J. Comput. Chem. 3 (1982) 214.
[37] M. Dupuis and H.F. King, J. Chem. Phys. 68 (1978) 3998.
[38] P. Nachtigall, K.D. Jordan and K.C. Janda (1991), submitted for publication.
[39] K.P. Huber and G. Herzberg, Molecular spectra and molecular structure, Vol. 4. Constants of diatomic molecules (Van Nostrand Reinhold, New York, 1979).
[40] C.J. Wu and E.A. Carter, to be submitted.